

BIOMECHANICS OF MUSCLES

K.M. Correia da Silva

Biomechanics Laboratory, Gulbenkian Institute of Science, Oeiras, Portugal.

INTRODUCTION

The skeletal muscles are the source of power for the mechanical peripherals of the central Nervous System (CNS) and our understanding of the mechanisms through which the CNS controls the skeletal muscles to achieve highly co-ordinated movements is still very limited. We approached this problem by considering the muscles as parallel and series combinations of a basic one-degree-of-freedom neuromuscular assemblage, the *mechanoeffector unit* (MU) whose structure and properties are defined. The laws of association of the MU's are such that the whole muscle has the same formal structure, albeit with different parameter values, as that of a single unit. This fact is taken advantage of to check the performance of the theoretical model against experimental muscle performance data. Only the dynamical response of the unit to small perturbations around a quiescent working point are considered so that linear approximations to its functional relationships may be used. This dynamical response is simulated numerically using published data on the characteristics of muscles and sensors and its capacity to meet requirements of (a) precision (b) stability (c) speed of response and (d) insensitivity to external loading is evaluated and checked with experimental known data. The role of the spinal cord in providing filtering circuitry to improve the mechanoeffector assemblage design and to achieve for it a configuration which fits well the known overall characteristics of its natural counterparts.

METHODS

The diagram of figure 1 illustrates the structure of the MU control assemblage which is based on the relevant experimental data not only in what concerns the functional structure which it implements but also in the parameter characteristics of its component elements. Two types of muscle fibres are considered, namely, the extrafusal fibres (EFF) which constitute the muscle contractile element and the intrafusal fibres (IFF) which are part of the muscle spindle sensorial structure. Two types of sensors are considered: the muscle spindle (MS) and the Golgi tendon organ (TO). F_1, F_2, F_3, F_4 are neural correcting filters located at spinal cord level and Δ is the propagation delay in the afferent nerve links and which account for both the afferent and efferent delays. The small signal variables are the as follows: muscle (u) and fusimotor (v) central commands, muscle (α) and fusimotor (γ) efferent commands, the

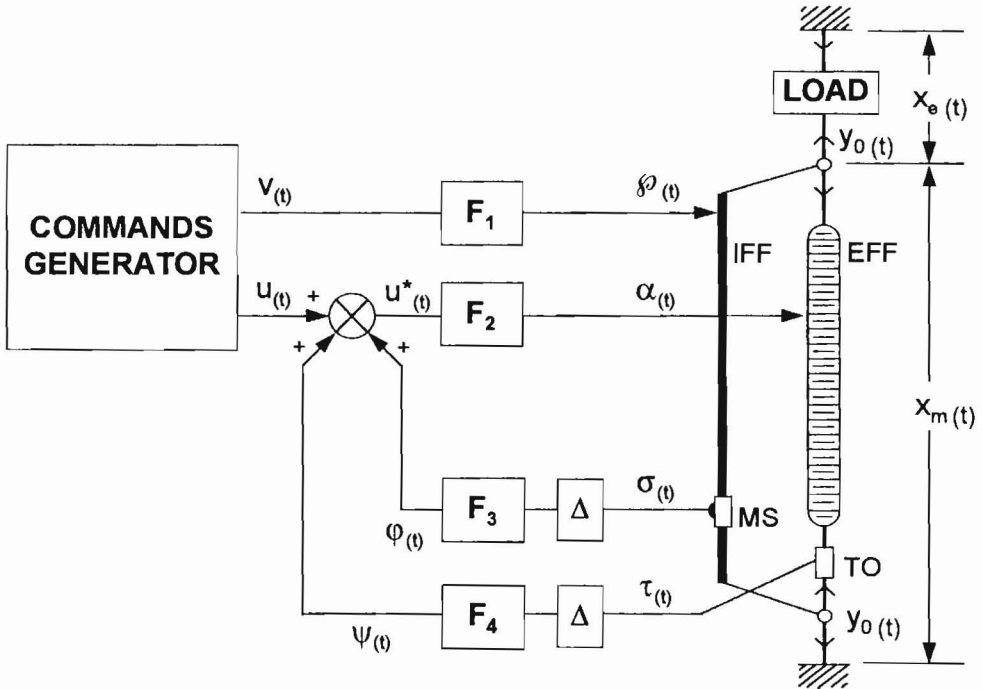


Fig.1 - Mechanoeffector Unit Control Assemblage.

afferent signals from the spindle (σ) and from the tendon organ (τ), the corresponding filtered signals (ϕ) and (ψ) and the length changes (or strains) of the EFF (x_m), of the external load (x_e) and of the overall MU assemblage ($x_0 = x_m = -x_e$); y_0 is the force (or stress) developed by the MU. The feedback relationships for the sensorial outputs are those which have been found to be most suitable for the optimization of the control assemblage. Actually, the feedback arrangements have reasonable experimental support and both have, separately or together, been considered by other authors (Stein, 1974): the length feedback from the MS is negative as a result of the differential assemblage of this sensor and the force feedback from the TO is positive. Feedback loops involving higher CNS areas are not considered and so the only propagation delay to be taken into account is that which occurs in the afferent pathways. The Commands Synthesizer represents the cerebral cortex areas which are responsible for generating the commands that control the MU. The fact that we consider only small incremental variations around quiescent working points allows the linearization of the functional relationships between the different elements of the MU assemblage and the use of the Laplace Transform formalism. The transfer functions of the EFF and of the TO and the MS are, respectively:

$$y_0(s) = C(s) \cdot \alpha(s) + Yg(s) \cdot x_0(s)$$

$$\tau(s) = A_T(s) \cdot y_0(s)$$

and

$$\sigma(s) = A_S(s) \cdot x_0(s) + B_S(s) \cdot \gamma(s) \quad (1)$$

where s is the Laplace variable, $C(s)$ is the complex frequency-to-force conversion factor, $Y_g(s)$ is the muscle stiffness and $A_T(s)$, $A_S(s)$ and $B_S(s)$ are transfer functions relating $\tau(s)$ to $y_0(s)$ and $\sigma(s)$ to $x_0(s)$ and to $\gamma(s)$. The controlled variables, namely, the output length (x_0), force (y_0) and elastance (Z_0) are expressed, in terms of the corresponding Laplace transforms, by the equations (2), (3) and (4):

$$x_0(s) = \frac{G(s)}{1 + G(s).H(s)} [u(s) + B_S^{**}(s).v(s)] + z_0(s).y_e(s) \quad (2)$$

$$y_0(s) = \frac{C^*(s)}{1 - C^*(s).A_T^*(s)} [u(s) + B_S^{**}(s).v(s)] - \frac{Y_g(s) + C^*(s).A_S^*(s)}{1 - C^*(s).A_T^*(s)} .x_0(s) \quad (3)$$

$$z_0(s) = \frac{1}{Y_e(s) + Y_g(s)} . \frac{1 - C^*(s).A_T^*(s)}{1 + G(s).H(s)} \quad (4)$$

where:

$$A_S^*(s) = e^{-\Delta s} . F_3(s) . A_S(s) \quad B_S^{**}(s) = e^{-\Delta s} . F_3(s) . B_S(s)$$

$$A_T^*(s) = e^{-\Delta s} . F_4(s) . A_T(s)$$

$$B_S^{**}(s) = F_1(s) . B_S(s) \quad C_S^*(s) = F_2(s) . C(s)$$

$$G(s) = \frac{C^*(s)}{Y_e(s) + Y_g(s)} \quad H(s) = A_S^*(s) - A_T^*(s) . Y_e(s) \quad (5)$$

$e^{-\Delta s}$ is the delay transfer function and $Y_e(s)$ is the external load stiffness.

RESULTS AND DISCUSSION

The parameters and relationships which characterize the muscle fibres properties and the mechanoreceptors parameters were obtained from the literature (Alnaes 1967; Bana et al., 1976; Jansen & Rudjord, 1964; Jewel & wilkie, 1958; Houk & Henneman, 1967;). Figure 2 represents the Nyquist Diagram (Palm, 1986) for to the MU. This diagram is the complex plane plot of the product $G(s).H(s)$, the MU open loop transfer function which occurs in the denominator of

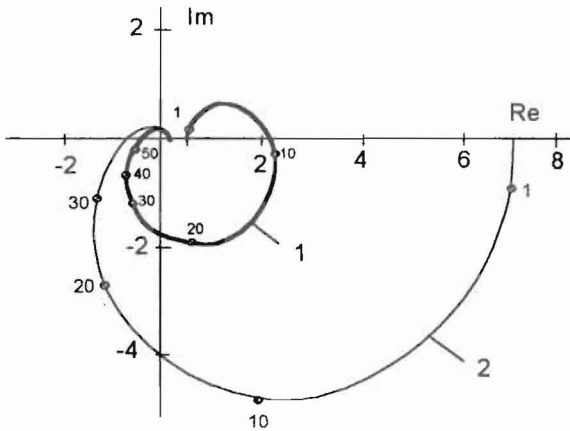


Fig. 2 - Nyquist Diagram in the complex (Re+jIm) plane. Numbers along the diagrams represent ω in rad sec^{-1} .

equation (2), when $s=j\omega$ and the angular frequency ω varies from zero to infinite. This diagram provides a powerful tool for the study of the system behaviour at low and high frequencies. When the plot passes through, or includes, the point $(-1+j0)$ the system becomes unstable. Diagram 1 refers to the situation when there is no filtering and corresponds to a position servomechanism of type zero. i.e., with no pole at the origin and therefore with a finite position error. Diagram 2 represents the same when the filters match the transfer function of the corresponding link, i.e., $F_1 = k_1 \cdot B_S^{-1}$, $F_2 = k_2 \cdot C_S^{-1}$, $F_3 = k_3 \cdot A_T^{-1}$, $F_4 = k_4 \cdot A_S^{-1}$ with the k 's adjusted adequately. For this situation, which corresponds to remove the frequency-dependent part of the sensors and effector characteristics, the dynamical behaviour of the MU is optimal and demonstrates the capacity of the nervous system to compensate for the biological material characteristics. This solution brings out clearly the role played by the two types of sensors. The MS controlling the MU length error and the TO controlling its output (Z_0) which is easily brought to small value found experimentally. The position error is minimized and the speed of response increased by the high transfer gains made possible by this filtering scheme and the various components of the MU performance become well consistent with those found experimentally.

REFERENCES

- Alnaes, E. (1967) *Acta Physiol. Scand.*, **70**, 176-187.
 Bana, P., A. Mannard & R.B. Stein (1976) *Biol. Cybernetics*, **22**, 129-137.
 Houk, J.C. & E. Hennemans (1967) *J. Neurophysiol.*, **30**, 466-481.
 Jansen, J.K.S. & T. Rudjord (1964) *Acta Physiol. Scand.*, **62**, 364-379.
 Jewel, B.R. & D.R. Wilkie (1958) *J. Physiol.*, **143**, 515-540.
 Palm, W.J. (1986) *Control Systems Engineering*, J. Wiley & Sons